Optical coherent manipulation of polariton modes and of their radiative decay

I. Kudyk,* T. Voss, I. Rückmann, and J. Gutowski
Institute for Solid State Physics, Semiconductor Optics Group, University of Bremen, P.O.Box 330440, 28334 Bremen, Germany

S. Schumacher† and F. Jahnke
Institute for Theoretical Physics, University of Bremen, P.O.Box 330440, 28334 Bremen, Germany

(Received 13 March 2006; published 26 June 2006)

The coherent optical control of polariton modes is studied in time-resolved pulse-transmission experiments on a ZnSe/ZnSSe heterostructure. Using a phase-locked pulse pair at low excitation intensity it is shown that the polariton modes, their quantum beat structure, and the radiative decay can be coherently manipulated. Calculations based on a microscopic polariton theory can explain the measured findings without the use of fit parameters. Additionally, the decay times of the coherent polarization, which depend on the involved polariton modes and their radiative decay, are extracted on the basis of a phenomenological model.

DOI: 10.1103/PhysRevB.73.235345 PACS number(s): 71.36.+c, 78.47.+p

I. INTRODUCTION

The coherent control of the excitonic polarization in semiconductor heterostructures has been a field of intense research in the last years.[1–12] It provides the possibility of manipulating elementary quantum-mechanical excitations on ultrashort time scales with regard to both their amplitudes and relative phases. The applications of coherent control are not only limited to fundamental studies of the carrier and polarization dynamics on ultrashort time scales, which are strongly governed by correlation effects. Coherent-control schemes are also prerequisites for the successful implementation of quantum-logic schemes in the strongly emerging field of quantum information processing.[13] For semiconductor quantum-well structures with large exciton binding energies and a significant spectral separation of heavy-hole and light-hole excitons, the excitation of one single excitonic transition is possible with ultrashort laser pulses even if they possess spectral bandwidths in the order of several to several tens of nanometers.

However, the situation is significantly complicated if the width of the quantum-well layer is increased up to dimensions of several exciton Bohr radii. Then, propagation effects strongly modify the light-matter interaction in the semiconductor heterostructure. One consequence is the occurrence of further resonances associated with so-called center-of-mass (COM) quantized exciton-polaritons.[14–16] In the active layer the k-vector in propagation direction, which is considered to be perpendicular to the wide-quantum-well layer, is quantized due to the finite thickness of the layer according to $k=n\pi/d$ (n integer, d layer thickness) provided that one assumes the simplified picture of decoupled exciton relative and COM motion. For layer thicknesses d in the range of a few exciton Bohr radii, this leads to several COM quantized exciton-polariton resonances being separated by a few millielectron volts, which are thus simultaneously excited by ultrashort laser pulses. Consequently, the coherent excitation of more than one excitonic resonance significantly complicates the response of the semiconductor system to the optical excitation.

This paper addresses the question how optical coherent-control schemes work in the system of multiple exciton-polariton resonances. A separate manipulation of the different polariton resonances in the low-density regime should be possible but has been analyzed neither experimentally nor theoretically thus far. In this paper, we present experimental studies and microscopic simulations of the optical coherent control of COM quantized exciton polariton modes in a ZnSe-based heterostructure. We find that under low excitation densities a separate manipulation of the different polariton modes can be achieved that results in strong modifications of the quantum-beat structure of the transient optical polarization. Additionally, we observe a significant change of the decay time of the coherent polarization, both in experiment and microscopic theory, as different polariton modes are amplified or diminished in the coherent control process. By use of a simple phenomenological model, we are able to quantify the contributions of the different polariton modes to the overall signal and to extract the decay time of the coherent polarization. The comparison to the simulations based on a microscopic theory reveals that the change of the decay time is due to the different radiative decay rates of the polariton modes being excited with different relative intensities in the coherent-control experiments.

II. EXPERIMENTAL SETUP

The coherent control of polariton modes is studied on a 25 nm ZnSe layer embedded in two 1 μm ZnSSe barriers. The sample was pseudomorphically grown by molecular-beam epitaxy on a (001) GaAs substrate. To realize the experiments in transmission geometry, the substrate was removed by chemical etching. The laser pulses were generated by a frequency-doubled mode-locked Ti:sapphire laser. The single pulses had a full width at half maximum (FWHM) of 120 fs at a repetition rate of 82 MHz. The selected spectral position ($\lambda \approx 440$ nm) and the spectral width of the pulses allowed for a simultaneous excitation of the first four heavy-hole exciton-polariton resonances labeled here as hh_1 to hh_4. To achieve coherent control, a phase-locked pulse pair was generated by use of an actively stabilized Michelson interferometer. The time delay between two phase-locked pulses was $t_{int}=t_{int}^0+\Delta t_{int}$. Here, t_{int}^0 denotes the basic temporal separation of the two phase-locked pulses in the femtosecond range. The fine tuning Δt_{int} was varied with an accuracy of

40 as. The time resolved measurements were performed using an up-conversion technique (UPC) for which the signal transmitted through the sample was spatially overlapped with an infrared reference pulse ($\lambda \approx 880$ nm) in a β-barium-borate crystal. The sum-frequency signal ($\lambda \approx 293$ nm) generated due to this overlap was detected by a photomultiplier. The reference pulse was temporally scanned over the transmitted signal by varying the time delay t_{UPC} between them. The time resolution of the UPC technique was measured to be 100 fs. All measurements were carried out at a temperature of 4 K.

III. MICROSCOPIC THEORY

According to the experimental setup, we consider a semiconductor layer in a slab geometry, with homogeneous extension in the x-y plane and with a finite spatial extension in the z direction.[16] For the optical excitation, a pair of incoming phase-coupled Gaussian light pulses propagating in the z direction is assumed to be generated by an external source outside the sample. As outlined in Ref. 17, Maxwell's equations are solved self-consistently together with the equation of motion for the induced material polarization $\mathbf{P}(z,t)=P(z,t)\mathbf{e}$ with the polarization vector $\mathbf{e}$ of the incoming electric field $\mathbf{E}(z,t)$. In the linear optical regime and for excitation near the band-gap energy, the semiconductor response to the external electromagnetic field is exclusively determined by the excitonic transition amplitude $p_{\mathbf{k}}(z_e,z_h,t)=\langle \psi^h_{\mathbf{k}}(z_h)\psi^e_{\mathbf{k}}(z_e)\rangle$ with the electron $\psi^e_{\mathbf{k}}(z_e)$ and hole $\psi^h_{\mathbf{k}}(z_h)$ annihilation operators. The transition amplitude is given as a function of the in-plane momentum $\mathbf{k}=(k_x,k_y)$ to make use of the in-plane homogeneity of the given system. The real-space formulation in the z direction allows to include the spatial inhomogeneity of the heterostructure. The macroscopic polarization of the system is given by

$$P(z,t)=\sum_{\mathbf{k}} d^*_{eh} p_{\mathbf{k}}(z,z,t), \tag{1}$$

with the local dipole matrix element $d_{eh}(z_e-z_h)=d_{eh}\delta(z_e-z_h)$ and the excitonic transition amplitude $p_{\mathbf{k}}(z_e,z_h,t)$ for equal electron and hole z coordinates. Using an expansion in terms of excitonic eigenstates $\phi_m(\mathbf{k},z_e,z_h)$, the equation of motion for the excitonic transition amplitude

$$p_{\mathbf{k}}(z_e,z_h,t)=\sum_m p_m(t)\phi_m(\mathbf{k},z_e,z_h) \tag{2}$$

leads to[18]

$$i\hbar\frac{d}{dt}p_m(t)=(\varepsilon_m-i\gamma)p_m(t)-d_{eh}\int\left[dzE(z,t)\sum_{\mathbf{k}}\phi^*_m(\mathbf{k},z,z)\right]. \tag{3}$$

Then, the time evolution of the excitonic polarization (1) can be determined by the equation of motion (3) for the coefficients $p_m(t)$. The source term for each coefficient $p_m(t)$ is given by the dipole coupling constant d_{eh} and the projection of the electric field amplitude $E(z,t)$ to the corresponding mth excitonic eigenstate $\phi_m(\mathbf{k},z_e,z_h)$. A phenomenological dephasing constant $\gamma=0.11$ meV for the excitonic polarization has been included, which is in accordance with the homogeneous broadening observed in Ref. 19 for a similar sample. The solution of the homogeneous part of Eq. (3) can be given in terms of damped, oscillating solutions for the coefficients $p_m(t)$ for each contributing eigenstate m with frequency $\omega_m=\varepsilon_m/\hbar$. The exciton eigenenergies ε_m and eigenfunctions $\phi_m(\mathbf{k},z_e,z_h)$ fulfill the eigenvalue equation

$$\sum_{\mathbf{k}'}\mathcal{H}^X_{\mathbf{k}\mathbf{k}'}\phi_m(\mathbf{k}',z_e,z_h)=\varepsilon_m\phi_m(\mathbf{k},z_e,z_h). \tag{4}$$

This eigenvalue equation is evaluated according to the microscopic physical boundary conditions of the system, so that the exciton wave functions vanish if either the electron or the hole reaches one of the semiconductor surfaces. These boundary conditions are exactly fulfilled for each single exciton wave function $\phi_m(\mathbf{k},z_e,z_h)$. This is in contrast to previous formulations[20,21] where an expansion in terms of bulk exciton wave functions with appropriate boundary conditions is used. In this case, the boundary conditions for the excitonic states are only approximately fulfilled. The excitonic Hamiltonian $\mathcal{H}^X_{\mathbf{k}\mathbf{k}'}$ for the slab geometry is given by

$$\mathcal{H}^X_{\mathbf{k}\mathbf{k}'}=(\varepsilon^e_{\mathbf{k},z_e}+\varepsilon^h_{\mathbf{k},z_h})\delta_{\mathbf{k}\mathbf{k}'}-V^{z_e z_h}_{\mathbf{k}\mathbf{k}'}. \tag{5}$$

The one-particle energy operators in effective-mass approximation are

$$\varepsilon^i_{\mathbf{k},z}=\frac{\hbar^2k^2}{2m^*_{i\|}}-\frac{\hbar^2}{2m^*_{iz}}\frac{\partial^2}{\partial z_i^2}+\frac{E_{\mathrm{gap}}}{2}+V^i_{\mathrm{ext}}(z_i), \tag{6}$$

where $i\in\{e,h\}$. Here $m^*_{e\|}$, m^*_{ez} and $m^*_{h\|}$, m^*_{hz} denote the effective electron and hole masses for in-plane ($\|$) and z direction, respectively. The external potential $V^i_{\mathrm{ext}}(z)$ is used to model the finite-height band offsets in the heterostructure, that are calculated along the guidelines in Ref. 16 with a sulfur content of 7% in the ZnS_xSe_{1-x} barrier material. The latter has been experimentally determined by x-ray diffraction measurements. The Coulomb matrix elements are given by

$$V^{zz'}_{\mathbf{k}\mathbf{k}'}=\frac{e_0^2}{2\varepsilon_0 n_{\mathrm{bg}}^2}\frac{e^{-|\mathbf{k}-\mathbf{k}'||z-z'|}}{|\mathbf{k}-\mathbf{k}'|}, \tag{7}$$

with $|\mathbf{k}-\mathbf{k}'|=\sqrt{k^2+k'^2-2kk'\cos(\phi_k-\phi_{k'})}$. Here e_0 is the electronic charge, ε_0 is the vacuum dielectric constant, and n_{bg} denotes the nonresonant background refractive index. All material parameters are taken from Ref. 16. For the investigated system, only excitons with in-plane s symmetry (rotational invariance around the z axis) are excited in linear optical experiments. This is taken into account by an in-plane angular momentum decomposition that yields the excitonic Hamiltonian (5) projected to the in-plane s subspace.[17,18] Furthermore, according to the experimentally excited and investigated spectral window, it is sufficient to include a finite number of the lowest-energy heavy-hole exciton states in the expansion (2).[16,18]

As mentioned above, the dynamics of the optically induced macroscopic polarization $P(z,t)=d^*_{eh}\Sigma_m[p_m(t)\Sigma_{\mathbf{k}}\phi_m(\mathbf{k},z,z)]$ is self-consistently coupled to the electromagnetic fields, which obey Maxwell's equations.

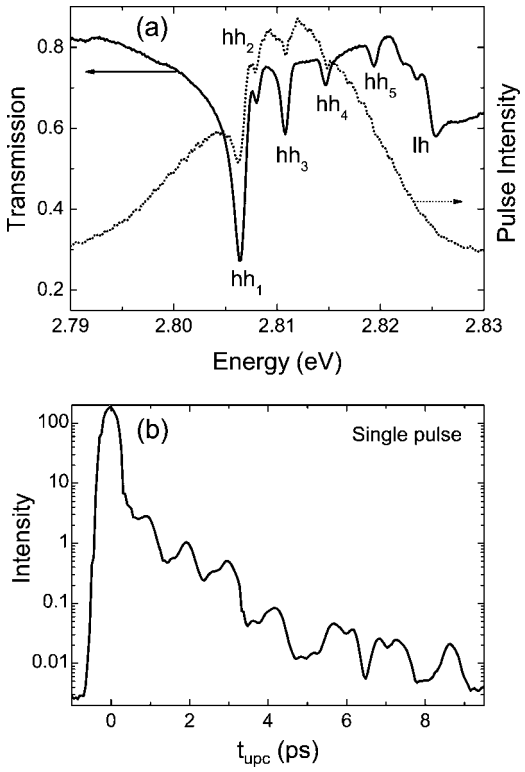

FIG. 1. (a): Linear transmission spectrum of 25 nm ZnSe heterostructure (solid line) and spectral profile of the excitation pulse (dotted line) after having passed through the sample. (b) Time resolved single-pulse transmission.

Therefore, in addition to the phenomenologically introduced dephasing constant γ in Eq. (3), the radiative decay[22,23] of the excitonic polarization is also correctly included in the theoretical description. The discussion of the radiative decay and the influence of the coherent control on the radiative decay times will be presented, in detail, in Sec. IV which devoted to the experimental and theoretical results.

IV. RESULTS AND DISCUSSION

A. Experiment and microscopic theory

The linear transmission spectrum of the 25 nm ZnSe heterostructure is shown as solid line in Fig. 1(a). The spectrum is dominated by a pronounced mode structure due to the COM quantization of the heavy-hole (hh) exciton polariton motion. On the high-energy side an absorption peak due to the light-hole (lh) exciton is seen. The dotted line in Fig. 1(a) shows the spectrum of the single laser pulse with low excitation energy of 0.1 pJ after having passed through the sample. It demonstrates that the coherent pulse excites the sample mainly in the spectral region of the resonances hh_1 to hh_4. The simultaneous coherent excitation of four polariton modes causes beat structures on the time resolved transients, shown in Fig. 1(b). For $t_{UPC} > 0.5$ ps, the beat structure is superimposed to the signal emitted by the decaying coherent polarization. The complicated nature of the beating behavior is caused by the overlay of different fundamental oscillating signals. The corresponding fundamental beat periods can be calculated according to

$$T_{beat} = h/\Delta E, \tag{8}$$

where ΔE is the energy splitting between two polariton modes. The energy differences between various polariton modes and the corresponding calculated fundamental beat periods are shown in Table I. Because of the large oscillator strength of the hh_1 ground mode, the beatings between the hh_1 mode and the higher modes (hh_2 to hh_4) dominate the modulation of the time-resolved signal in Fig. 1(b). The beatings between the higher modes (the last three beat periods in Table I) are insignificant due to their negligible oscillator strengths in comparison to that of the hh_1 ground mode.

TABLE I. Experimental (according to Fig. 1(a)) and theoretical (according to Fig. 4(c)) energy differences between polariton modes, and corresponding calculated beat periods.

Interfering modes	ΔE (meV) Experimental	T_{beat} (ps) Experimental	ΔE (meV) Theoretical	T_{beat} (ps) Theoretical
hh_1-hh_2	1.65	2.51	1.64	2.52
hh_1-hh_3	4.45	0.93	4.37	0.95
hh_1-hh_4	8.28	0.50	7.92	0.52
hh_2-hh_3	2.8	1.48	2.73	1.52
hh_2-hh_4	6.63	0.62	6.28	0.66
hh_3-hh_4	3.83	1.08	3.55	1.17

Fröhlich *et al.*[24] first observed 1*s*-exciton-polariton beats with increasing period due to the interference of ordinary and extraordinary waves propagating in CuO_2. The origin of the beats reported here are interferences of the coherent polarizations of polariton states of the lower polariton branch created by the *k*-quantization. The hh-exciton polariton modes can be regarded as a system of resonances with a common ground state. Using a phase-locked pulse pair, the polariton mode polarizations can be manipulated. It is expected that the beat structure, which modulates the time-resolved signal, strongly depends on the delay time between the phase-locked pulses. To achieve a situation for which the beating between the hh_1 and hh_3 modes (these modes have larger oscillator strengths than all the other modes) can be effectively coherently controlled, the basic delay time t_{int}^0 was adjusted to 450 fs corresponding to half the hh_1-hh_3 beat period. In order to perform the coherent control, the fine-tuning delay Δt_{int} was varied over a range of a few femtoseconds. For different values of Δt_{int}, time-resolved transients were measured; see Fig. 2(a). The signal intensity is encoded in a logarithmic gray scale. For comparison, calculated time-resolved signals based on the microscopic theory are shown in Fig. 2(b). The calculated transients exhibit the same behavior as found in the experiment with respect to the intensity decay over three orders of magnitude as well as regarding the oscillation periods observable along the Δt_{int} axis. Because of the limited contrast achievable in the experiment the measured contrast ratio is smaller than the theoretical one. However, it can clearly be stated that the microscopic

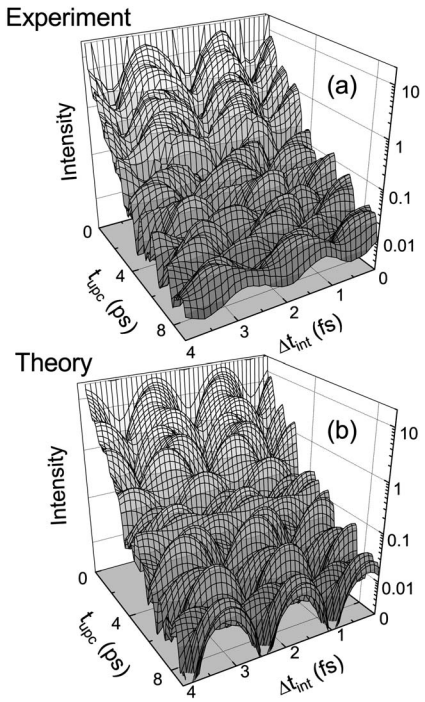

FIG. 2. Three dimensional plots of the time-resolved transmitted intensity as a function of the fine-tuning delay Δt_{int} between the two phase-locked pulses for $t_{\mathrm{int}}^{0}=450$ fs: (a) Experiment and (b) microscopic theory.

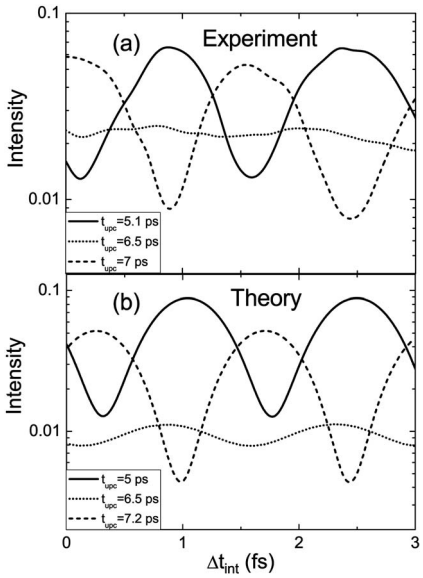

FIG. 3. Cuts from Fig. 2 at different t_{UPC}: (a) experiment and (b) microscopic theory.

model reproduces the measured features very well without use of fitting parameters.

In Figs. 2(a) and 2(b) cuts along the Δt_{int} axis for fixed t_{UPC} represent so-called switching curves, which show oscillations due to the continuous change between constructive and destructive interference of the coherent polarization in dependence on the fine tuning. The oscillation period is given by that of the polariton modes according to $T=h/E_{hh}$ ($T\approx 1.5$ fs). The switching curves observed for different t_{UPC} values exhibit different phases and contrast ratios as it is demonstrated for three typical examples in Fig. 3. The signals for $t_{\mathrm{UPC}}\approx 5$ ps (solid lines) and $t_{\mathrm{UPC}}\approx 7$ ps (dashed lines) display opposite phases, while the switching curve at $t_{\mathrm{UPC}}=6.5$ ps (dotted lines) shows a strongly reduced contrast ratio. It is remarkable that the contrast ratio at $t_{\mathrm{UPC}}\approx 7$ ps is larger than that at $t_{\mathrm{UPC}}\approx 5$ ps and thus exhibits an oscillating behavior as a function of t_{UPC}. This observation can be explained through the complex beating between the four polariton modes, which leads to a subsequent switch-on and -off of the polarization of the different modes involved along the variation of Δt_{int}.

The change of the beat structures in dependence on Δt_{int} is clearly seen by looking at cuts along the t_{UPC} axis in the 3D-plot of Fig. 2. In Figs. 4(a) and 4(b), measured (solid lines) and calculated (dotted lines) transients extracted from the three-dimensional (3D) plots at two fine-tuning delays Δt_{int} are exemplarily compared. The beatings between the involved polariton modes are superimposed to the signal of the decaying coherent polarization. The variations in the modulation observed in the transients result from polariton beats that are different in both cases. The comparison of the measured transients without [Fig. 1(b)] and with coherent control [Figs. 4(a) and 4(b)] demonstrates that the beat structure is strongly manipulated by the phase-locked pulse pair.

The Fourier transforms of the transients yield the spectra of the transmitted phase-locked pulse pair and provide direct information about the excitation of particular polariton modes. Figure 4(c) shows the Fourier spectra calculated with the microscopic theory. It can be seen that the shape of the spectra and thus the magnitude of the absorption at particular polariton resonances strongly depends on the time delay between the phase-locked pulses. In the spectrum calculated for $\Delta t_{\mathrm{int}}=0.3$ fs (solid line), the hh_1, hh_4 polariton modes are diminished and the hh_2 mode is completely suppressed by the phase-locked pulse pair. In contrast, in the spectrum calculated for $\Delta t_{\mathrm{int}}=0.6$ fs (dotted line), the hh_3 polariton mode only is suppressed.

According to this discussion, the experimental and theoretical transients at $\Delta t_{\mathrm{int}}=0.3$ fs [Fig. 4(a)] are dominated by the beat period $T_{\mathrm{beat}}\approx 1$ ps corresponding to the $\mathrm{hh}_1-\mathrm{hh}_3$ and $\mathrm{hh}_3-\mathrm{hh}_4$ beatings (see Table I). The other beat period $T_{\mathrm{beat}}\approx 0.5$ ps related to the hh_1-hh_4 beating is observed as small "humps" on the transients. The $\mathrm{hh}_1-\mathrm{hh}_4$ beat period is less well observable on the measured than on the calculated transient. The hh_2 mode is suppressed strongly by the phase-locked pulse pair.

The transients for $\Delta t_{\mathrm{int}}=0.6$ fs are shown in Fig. 4(b). They exhibit a superposition of two beat structures with beat periods $T_{\mathrm{beat}}\approx 3$ ps and $T_{\mathrm{beat}}\approx 0.5$ ps, corresponding to the $\mathrm{hh}_1-\mathrm{hh}_2$ and $\mathrm{hh}_1-\mathrm{hh}_4$ interferences, respectively (see Table I). Here, in contrast to the case of $\Delta t_{\mathrm{int}}=0.3$ fs, the hh_3 mode is suppressed by the phase-locked pulses. For both cases, the experimental and theoretical transients clearly demonstrate the selective coherent control of the polarization of polariton modes.

It seems that in all cases the hh_1 ground mode is more or less involved in the beat structure due to its dominating oscillator strength. Even for the case of the hh_1 ground mode

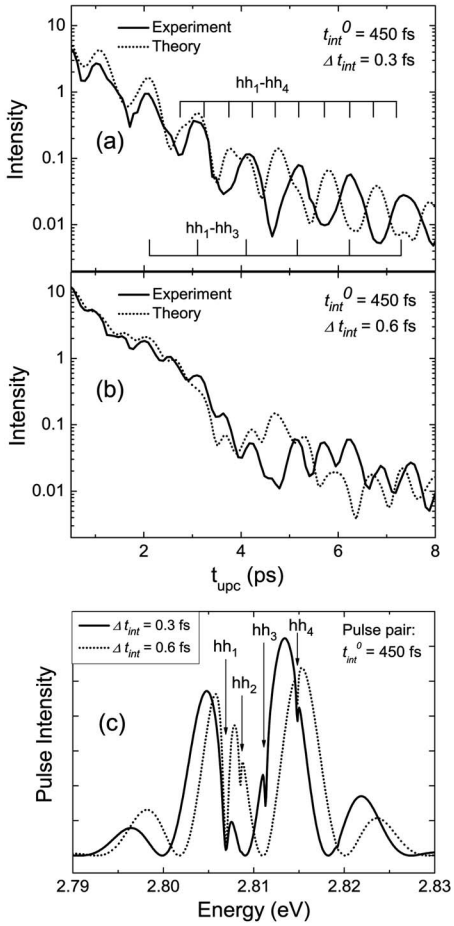

FIG. 4. (a,b) Time-resolved transients at $\Delta t_{\mathrm{int}}=0.3$ fs (a) and $\Delta t_{\mathrm{int}}=0.6$ fs (b). Solid line: experiment. Dashed line: microscopic theory. (c): Calculated spectra of the phase-locked pulse pair after having passed through the sample at $\Delta t_{\mathrm{int}}=0.3$ fs (solid line) and $\Delta t_{\mathrm{int}}=0.6$ fs (dashed line).

diminished by the phase-locked pulses [solid line in Fig. 4(c)], its magnitude is still sufficient for a distinct contribution to the beat structure.

Figures 4(a) and 4(b) show a good agreement between the measured and microscopically calculated transients with respect to the polarization decay and to the beat amplitudes. Regarding the beat periods, the microscopic calculations well reproduce the experimental findings over two orders of pulse-transmission intensity up to $t_{\mathrm{UPC}}\approx 4$ ps. After this time, a phase shift occurs between the measured and the calculated beat periods. We attribute this deviation to the fact that the linear transmission of the ZnSe/ZnSSe sample is further influenced by the ZnSSe cladding layers, which form an outer Fabry-Perot resonator for the optical field. Furthermore, the outer sample-air surface might slightly modify the transmission spectra and, hence, the beat structure. The influence of the ZnSSe barriers on the polariton resonances is not taken into account to simplify in the microscopic calculations. Therefore, the amplitudes of various modes can differ between experiment and calculations. For example, the calculated spectrum of the pulse pair for $\Delta t_{\mathrm{int}}=0.3$ fs [solid line in Fig. 4(c)] demonstrates the excitation of the hh_4 polariton mode, and the corresponding calculated transient [dotted line in Fig. 4(a)] shows the $\mathrm{hh}_1-\mathrm{hh}_4$ beating superimposed to the $\mathrm{hh}_1-\mathrm{hh}_3$ one. In the experiment, the absorption at the hh_4 polariton mode may have been diminished by the Fabry-Perot effect, and the $\mathrm{hh}_1-\mathrm{hh}_4$ beat structure is not observed [Fig. 4(a), solid line]. Nevertheless, a good agreement is achieved between experimental and microscopically calculated curves.

B. Experiment and phenomenological model

To allow for additional and more intuitive insight into the contributions of the different polariton modes to the overall signal, we use a phenomenological model to fit the transients and to extract the decay time of coherence. Within this model, it is also fairly easy to obtain simple quantitative numbers of the mode amplitudes involved for the different two-pulse interference cases. Because of the changes of the beat structures in dependence on Δt_{int}, it is difficult to extract the polarization decay directly from the measured transients. The knowledge of the polarization decay time allows one to discuss the influences of dephasing and of radiative decay. The phenomenological model starts from the damped oscillations of the coherent polarization P_i of an excited mode with resonance energy E_i. The real part is written as

$$P_i(t) = A_i e^{-(t/\tau)} \cos(\omega_i t), \tag{9}$$

with the mode frequency $\omega_i=E_i/\hbar$, the mode amplitude $A_i=\sqrt{S_i}$ (with S_i being the area under the corresponding absorption peak of the polariton resonance, i.e., the oscillator strength), and τ the decay time of the coherent polarization. The coherent polarization decay of all excited modes can be described for the low-excitation case as a linear superposition of the four involved polariton modes, assuming the same damping and the same phase for all excited modes. The measured time resolved pulse-transmission intensity I is proportional to the square of the induced polarization,

$$I(t) \propto e^{-(2t/\tau)} \sum_{i=1}^{4} [A_i \cos(\omega_i t)]^2. \tag{10}$$

If the coherent-control technique is applied to enhance or suppress selected polariton modes, the relative values of the mode amplitudes A_i change and therefore strongly depend on the delay time t_{int} between the phase-locked pulses.

The oscillator strengths of the resonances hh_1 to hh_4 can be experimentally determined from the linear transmission spectrum of the sample [Fig. 1(a), solid line]. From a fit with Lorentz lines, we obtain $S_1:S_2:S_3:S_4=1:0.09:0.4:0.23$. To reproduce the transient measured with coherent control at $\Delta t_{\mathrm{int}}=0.3$ fs, where both the hh_2 and hh_4 polariton modes are suppressed by the phase-locked pulse pair, the relative absorption of these modes is taken as being tenfold smaller with respect to their original values. This assumption is based on the experimentally achievable contrast between the constructive and destructive interference cases. For the simulation of the transient measured at $\Delta t_{\mathrm{int}}=0.6$ fs where only the hh_3 polariton mode is suppressed, this mode is taken as being tenfold smaller than its original value. The relative

TABLE II. Relative mode amplitudes without coherent control (according to Fig. 1), and with coherent control for $\Delta t_{\mathrm{int}}=0.3$ fs and for $\Delta t_{\mathrm{int}}=0.6$ fs.

Relative mode amplitude	Without coherent control	With coherent control	
		$\Delta t_{\mathrm{int}}=0.3$ fs	$\Delta t_{\mathrm{int}}=0.6$ fs
A_1	$\sqrt{S_1}=1$	$\sqrt{S_1}=1$	$\sqrt{S_1}=1$
A_2	$\sqrt{S_2}=0.3$	$\sqrt{0.1S_2}=0.09$	$\sqrt{S_2}=0.3$
A_3	$\sqrt{S_3}=0.63$	$\sqrt{S_3}=0.63$	$\sqrt{0.1S_3}=0.2$
A_4	$\sqrt{S_4}=0.48$	$\sqrt{0.1S_4}=0.15$	$\sqrt{S_4}=0.48$

mode amplitudes A_i without and with coherent control are shown in Table II.

The dotted curves in Fig. 5 show respective calculations using Eq. (10) and demonstrate good agreement with the experiment regarding the polarization decay and the beat periods. Since the calculated beat amplitudes strongly depend on the relation between the mode amplitudes, the deviation in Fig. 5(b) may be due to uncertainties in the estimation of the amplitude of the suppressed mode. Moreover, it is expected that deviations increase if more interfering mode polarizations are involved.

By use of the phenomenological model, the decay time of the coherent polarization is estimated to be $\tau=2.6$ ps for the transient at $\Delta t_{\mathrm{int}}=0.3$ fs [dotted line in Fig. 5(a)]. A smaller value of $\tau=2$ ps was found for the transient measured at $\Delta t_{\mathrm{int}}=0.6$ fs [dotted line in Fig. 5(b)]. The polarization decay time τ consists of two contributions, one being due to dephasing and the other due to the radiative decay of the coherent polarization. A mode with a larger oscillator strength has a faster radiative decay. Thus, suppression of such a mode causes a slower decay of the coherent polarization. As has been already stated in Sec. IV A, the hh_1 ground mode possesses a dominant influence on the coherent polarization decay due to its dominating oscillator strength. The calculated spectra of the phase-locked pulse pair in Fig. 4(c) show that the absorption at the hh_1 ground mode is weakened for $\Delta t_{\mathrm{int}}=0.3$ fs (solid line) in comparison to the case $\Delta t_{\mathrm{int}}=0.6$ fs (dotted line). This explains the longer coherence decay time for the former case. This result can be understood in the framework of the fully microscopic theory assuming the same dephasing while different radiative decay times of various polariton modes follow within the self-consistent treatment.

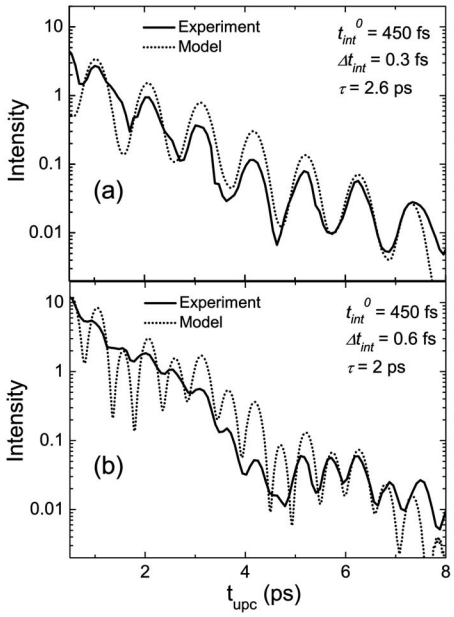

FIG. 5. Real-time resolved transients at (a) $\Delta t_{\mathrm{int}}=0.3$ fs and (b) $\Delta t_{\mathrm{int}}=0.6$ fs. Solid line: experiment. Dashed line: phenomenological model.

V. CONCLUSION

In this paper we have presented a demonstration of the coherent control of the polarizations of the heavy-hole exciton-polariton modes and their beatings in time-resolved pulse-transmission experiments using a phase-locked pulse pair, which is of interest for further applications as well as for studying the polariton dynamics. This method was successfully used to switch the polarizations of selected polariton modes and to manipulate the corresponding quantum beat structures in the transients. A microscopic polariton model that avoids additional boundary conditions was used to successfully simulate the experimental results. The model takes into account both dephasing and radiative decay for the determination of the coherence decay time. Therefore, it is expected that the coherent manipulation of involved modes results in a change of the coherence decay time. The simulations are in good agreement with the observed behavior of the measured coherent switching curves and with the measured transients over a range of two orders of magnitude of the intensity. Moreover, the polarization decay and beat amplitudes of the transients measured and calculated are in good agreement, too. Small deviations and a phase shift after 4 ps may be due to the influence of the outer Fabry-Perot resonator formed by the cladding layers, which was not taken into account in the microscopic polariton model. Additionally, a phenomenological model was used to extract the polarization decay times from the coherently controlled transients. To simulate the coherent control of polariton modes, the amplitude values of the suppressed modes were reduced by a factor of 10, as obtained from the experiment. If the $\mathrm{hh}_1-\mathrm{hh}_3$ interference dominates the transient, the hh_1 mode is slightly diminished and the hh_2 and hh_4 modes are suppressed, the polarization coherence decay time was found to be $\tau=2.6$ ps. If the $\mathrm{hh}_1-\mathrm{hh}_2$ and $\mathrm{hh}_1-\mathrm{hh}_4$ interferences occur on the transient, and only the hh_3 mode is suppressed completely, the decay time was found to be $\tau=2$ ps. The results clearly show that decay time of the coherent polarization and, hence, the radiative decay of the ensemble of excited polariton modes can be coherently manipulated.

ACKNOWLEDGMENTS

We acknowledge a grant for CPU time from the John von Neumann Institute for Computing at the Forschungszentrum Jülich and thank D. Hommel, University of Bremen, for providing the sample. I.K. acknowledges financial support from the Heinrich Böll Foundation.

*Electronic address: ikudyk@ifp.uni-bremen.de
†Present address: College of Optical Sciences, University of Arizona, Tucson, Arizona 85721, USA.

[1] A. P. Heberle, J. J. Baumberg, and K. Köhler, Phys. Rev. Lett. **75**, 2598 (1995).
[2] X. Marie, P. Le Jeune, T. Amand, M. Brousseau, J. Barrau, M. Paillard, and R. Planel, Phys. Rev. Lett. **79**, 3222 (1997).
[3] X. Marie, P. Renucci, S. Dubourg, T. Amand, P. Le Jeune, J. Barrau, J. Bloch, and R. Planel, Phys. Rev. B **59**, R2494 (1999).
[4] N. Garro, S. P. Kennedy, A. P. Heberle, and R. T. Phillips, Phys. Status Solidi B **221**, 385 (2000).
[5] P. Renucci, M. Paillard, X. Marie, T. Amand, J. Barrau, and C. Ciuti, Phys. Status Solidi A **178**, 373 (2000).
[6] D. S. Yee, K. J. Yee, S. C. Hohng, D. S. Kim, T. Meier, and S. W. Koch, Phys. Rev. Lett. **84**, 3474 (2000).
[7] J. Erland, V. G. Lyssenko, and J. M. Hvam, Phys. Rev. B **63**, 155317 (2001).
[8] K. Komori, T. Sugaya, M. Watanabe, and T. Hidaka, Jpn. J. Appl. Phys., Part 1 **39**, 2347 (2000).
[9] K. Komori, G. Hayes, T. Okada, B. Deveaud, X.-L. Wang, M. Ogura, and M. Watanabe, Jpn. J. Appl. Phys., Part 1 **41**, 2660 (2002).
[10] H. G. Breunig, T. Voss, I. Rückmann, J. Gutowski, V. M. Axt, and T. Kuhn, J. Opt. Soc. Am. B **20**, 1769 (2003).
[11] T. Voss, H. G. Breunig, I. Rückmann, and J. Gutowski, Phys. Rev. B **69**, 205318 (2004).
[12] T. Voss, I. Rückmann, J. Gutowski, V. M. Axt, and T. Kuhn, Phys. Rev. B **73**, 115311 (2006).
[13] X. Li, Y. Wu, D. Steel, D. Gammon, T. H. Stievater, D. S. Katzer, D. Park, C. Piermarocchi, and L. J. Sham, Science **301**, 809 (2003).
[14] U. Neukirch and K. Wundke, Phys. Rev. B **55**, 15408 (1997).
[15] H. P. Wagner, A. Schätz, R. Maier, W. Langbein, and J. M. Hvam, Phys. Rev. B **57**, 1791 (1998).
[16] S. Schumacher, G. Czycholl, F. Jahnke, I. Kudyk, H. I. Rückmann, J. Gutowski, A. Gust, G. Alexe, and D. Hommel, Phys. Rev. B **70**, 235340 (2004).
[17] H. C. Schneider, F. Jahnke, S. W. Koch, J. Tignon, T. Hasche, and D. S. Chemla, Phys. Rev. B **63**, 045202 (2001).
[18] S. Schumacher, G. Czycholl, and F. Jahnke, Phys. Status Solidi B **234**, 172 (2002).
[19] M. Seemann, F. Kieseling, H. Stolz, R. Franz, G. Manzke, K. Henneberger, T. Passow, and D. Hommel, Phys. Rev. B **72**, 075204 (2005).
[20] A. D'Andrea and R. Del Sole, Phys. Rev. B **25**, 3714 (1982).
[21] E. A. Muljarov and R. Zimmermann, Phys. Rev. B **66**, 235319 (2002).
[22] F. Jahnke, M. Kira, and S. W. Koch, Z. Phys. B: Condens. Matter **104**, 559 (1997).
[23] L. C. Andreani, G. Panzarini, A. V. Kavokin, and M. R. Vladimirova, Phys. Rev. B **57**, 4670 (1998).
[24] D. Fröhlich, A. Kulik, B. Uebbing, A. Mysyrowicz, V. Langer, H. Stolz, and W. von der Osten, Phys. Rev. Lett. **67**, 2343 (1991).